PHOTONICS Research

Structured laser beams: toward 2-μm femtosecond laser vortices

Yongguang Zhao,[1,2,*] Li Wang,[2] Weidong Chen,[2] Pavel Loiko,[3] Xavier Mateos,[4] Xiaodong Xu,[1] Ying Liu,[1] Deyuan Shen,[1] Zhengping Wang,[5] Xinguang Xu,[5] Uwe Griebner,[1] and Valentin Petrov[1]

[1]Jiangsu Key Laboratory of Advanced Laser Materials and Devices, School of Physics and Electronic Engineering, Jiangsu Normal University, Xuzhou 221116, China
[2]Max Born Institute for Nonlinear Optics and Short Pulse Spectroscopy, 12489 Berlin, Germany
[3]Centre de Recherche sur les Ions, les Matériaux et la Photonique (CIMAP), UMR 6252 CEA-CNRS-ENSICAEN, Université de Caen, Caen 14050, France
[4]Universitat Rovira i Virgili (URV), Física i Cristal·lografia de Materials i Nanomaterials (FiCMA-FiCNA), Marcel.li Domingo 1, 43007 Tarragona, Spain
[5]State Key Laboratory of Crystal Materials and Institute of Crystal Materials, Shandong University, Jinan 250100, China
*Corresponding author: yongguangzhao@yeah.net

Received 23 October 2020; revised 7 January 2021; accepted 12 January 2021; posted 12 January 2021 (Doc. ID 413276); published 22 February 2021

Structured ultrashort-pulse laser beams, and in particular eigenmodes of the paraxial Helmholtz equation, are currently extensively studied for novel potential applications in various fields, e.g., laser plasma acceleration, attosecond science, and fine micromachining. To extend these prospects further, in the present work we push forward the advancement of such femtosecond structured laser sources into the 2-μm spectral region. Ultrashort-pulse Hermite– and Laguerre–Gaussian laser modes both with a pulse duration around 100 fs are successfully produced from a compact solid-state laser in combination with a simple single-cylindrical-lens converter. The negligible beam astigmatism, the broad optical spectra, and the almost chirp-free pulses emphasize the high reliability of this laser source. This work, as a proof of principle study, paves the way toward few-cycle pulse generation of optical vortices at 2 μm. The presented light source can enable new research in the fields of interaction with organic materials, next generation optical detection, and optical vortex infrared supercontinuum.

https://doi.org/10.1364/PRJ.413276

1. INTRODUCTION

The term structured laser beam (SLB) generally refers to beams with spatially structured amplitude, phase, or polarization. Solving the scalar paraxial Helmholtz equation in Cartesian or cylindrical coordinates, one can derive the Hermite–Gaussian ($HG_{n,m}$) and Laguerre–Gaussian ($LG_{p,l}$) modes, respectively [1]. These eigenmodes, except for the lowest-order TEM_{00} mode, represent themselves SLBs capable of synthesizing other more complex SLBs by coherent or incoherent superposition. Utilizing the longitudinal electric-field component of a focused $HG_{n,m}$ beam, acceleration of particles is possible [2] and the trapping force in electron acceleration can be even higher compared to the fundamental mode [3]. For $LG_{p,l}$ modes with a topological charge of $l \neq 0$, a singularity point, i.e., optical vortex, appears, associated with vanishing amplitude and undefined phase. Such vortices with zero central intensity carry orbital angular momentum of $l\hbar$ per photon [4] and enable $LG_{p,l}$ beams to exert additional torques and forces on particles in optical trapping and manipulation [5], expand transmission capacity by exploiting a new degree of freedom in optical communications [6], break the diffraction resolution barrier in fluorescence light microscopy in combination with the stimulated emission depletion technique [7], and involve multi-dimensional states in quantum entanglement [8]. Femtosecond pulse optical vortices exhibiting higher critical power for self-focusing collapse compared to a conventional flattop beam [9], are attractive for some novel applications such as generation of attosecond vortices through high-order harmonic generation (HHG) [10], control of light filamentation for transporting and manipulating microwave radiation in air [11], and fabrication of three-dimensional chiral microstructures [12]. So far, the pulse durations of pulsed optical vortices in the 2-μm spectral region are much longer than 100 fs, thus limiting some potential applications related not only to the specific advantages due to the driving wavelength, e.g., in HHG or organic material processing, but also to the availability of better nonlinear materials for frequency conversion to yet longer (mid-IR) wavelengths.

Common methods used for generation of femtosecond optical vortices are based on transformation of a pre-existing ultrashort-pulse TEM_{00} mode by conventional phase modulation elements, including computer-generated holograms (CGHs) [13,14], spiral phase plates (SPPs) [15,16], and spatial light modulators (SLMs) [17]. Usually CGHs introduce extensive angular dispersion which inevitably results in spatial intensity distortion and temporal pulse broadening, so that complex $4f$ [13,18] or $2f$–$2f$ [14] compressors with additional diffraction gratings are required at the expense of conversion efficiency. SPPs do not produce spatial chirp but introduce topological-charge dispersion due to the high wavelength sensitivity [15], and SLMs generally suffer from low laser damage threshold and high cost [17]. Most importantly, all these methods are not suitable for creating ultrashort-pulse optical vortices in the 2-μm spectral range either because of the lack of suitable materials or bandwidth limitations. Alternatively, $HG_{n,m}$ modes can be transformed into $LG_{p,l}$ modes through rephasing their decomposed terms using "$\pi/2$ converters," e.g., single [19] or double cylindrical lenses [20], or two spherical-concave mirrors [21], which ensure a broadband operation range, high mode purity, and high laser damage threshold at lower cost.

Femtosecond pulse $HG_{n,m}$ modes can be directly generated from a mode-locked solid-state laser, as first observed in a Kerr-lens mode-locked Ti:sapphire laser as early as 1991, but in the form of a "mixed" spatial mode [22]. In 2009, pure high-order $HG_{0,m}$ modes were generated from a picosecond self-mode-locked Nd-laser and subsequently converted to LG_{01} modes [23], and recently the pulse duration near 1 μm was shortened to the 200-fs range employing an Yb-glass laser [24]. However, in the 2-μm spectral range, the pulse durations of lasers with HG_{01} and thus LG_{01} modes demonstrated so far were only in the sub-picosecond range and the spectral extent was correspondingly narrower [25,26].

Thus, the state of the art of ultrashort-pulse SLBs in the 2-μm spectral range and their promising applications motivated us to extend the studies to the femtosecond temporal regime. Here, we demonstrate a tabletop laser source that produces ultrashort-pulse HG_{10} and $LG_{0,m}$ modes both with pulse durations in the 100 fs range. The advantages of such a laser system over the traditional methods for generation of ultrashort-pulse SLBs are experimentally confirmed by characterizing the spatial beam pattern as well as temporal and spectral features. This work paves the route toward few-cycle pulse generation of optical vortices in the 2-μm spectral range. The generated pulsed optical vortices with such a short duration and broad optical spectrum will enable applications such as organic materials machining, novel molecular spectroscopy, and optical vortex infrared supercontinuum generation.

2. DESIGN AND METHOD

A standard, astigmatically compensated X-shape cavity was employed for producing the femtosecond HG_{10} beam through off-axis pumping. The gain medium was a 3% (atomic fraction) Tm^{3+}-doped $(Lu_{0.5}Y_{0.5})_2O_3$, i.e., Tm:$LuYO_3$ mixed ceramic with dimensions of 3 mm × 3 mm × 3 mm, water-cooled to 14°C in a Cu-holder. Compositional disorder of the used mixed ceramic enables broader and smoother gain spectra as compared to the parent compounds, thus supporting ultrashort pulse generation. To circumvent the etalon effect, the polished but uncoated ceramic sample was placed in the cavity at Brewster's angle which fixed the linear output polarization. As shown in Fig. 1, the 795 nm pump beam emitted from a tunable continuous-wave (CW) Ti:sapphire laser was focused by a lens ($f = 70$ mm) to a beam radius of 30 μm in the ceramic. M1 and M2 were two concave mirrors both with radius of curvature (RoC) of −100 mm. The passive mode-locking element was an uncoated GaSb-based semiconductor saturable absorber mirror (SESAM) with two quantum wells and photoluminescence at 2.09 μm [27]. A concave chirped mirror (CM1, RoC of −100 mm) was used to create a second beam waist on the SESAM to achieve the required saturation regime. Two additional plane chirped mirrors (CM2, CM3) providing the same group delay dispersion (GDD) of −125 fs^2 per bounce as CM1 served to manage the cavity dispersion. Because of the negligible group velocity dispersion of $LuYO_3$ [28], the total round-trip GDD was mainly dependent on the CMs and amounted to −1200 fs^2 at 2.07 μm with four beam bounces on CM2 and CM3 per round trip. The total optical cavity length amounted to ∼2 m. The output coupler (OC) employed was a plane-wedged mirror with a transmission of 0.5%.

Subsequently, the emitted HG_{10} laser beam of the mode-locked laser was externally converted into $LG_{0,\pm1}$ modes by a simple single-cylindrical-lens (SCL) converter [19]. A lens

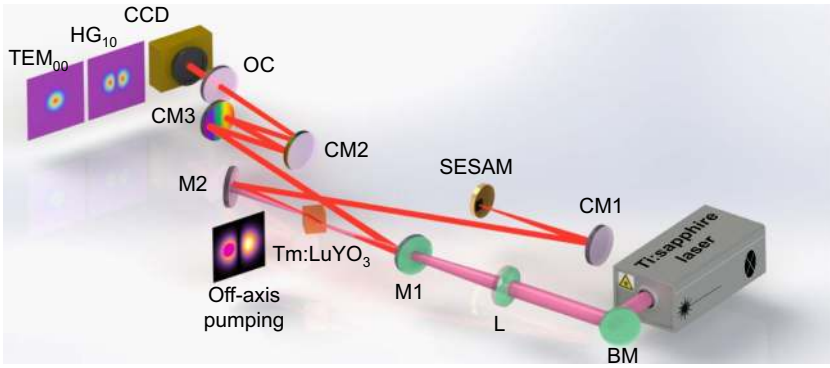

Fig. 1. Schematic of the passively mode-locked femtosecond TEM_{00} and HG_{10} laser using collinear and off-axis pumping (BM, bending mirror; L, lens; CM1–CM3, chirped mirrors; OC, output coupler).

of $f = 100$ mm was used to create a beam waist with a Rayleigh range (Z_R) of ~35 mm, followed by a cylindrical lens with $f_c = 35$ mm, placed exactly at Z_R behind the waist (see Section 3.C). The cylindrical lens was rotated by ±45° in the XY-plane to introduce a total Gouy-phase difference of $\Delta\Psi$ between the X- and Y-directions, where $\Delta\Psi$ can be expressed as [29]

$$\Delta\Psi = \pm[\pi/2 + \arctan(Z/Z_R - 1)] \mp [\arctan(Z/Z_R + 1)]. \quad (1)$$

If $Z \gg Z_R$, the phase difference will tend to $\pm\pi/2$, thus converting the femtosecond HG_{10} to $LG_{0,\pm1}$ modes. A CCD camera placed roughly 50 cm behind the cylindrical lens was used to record the LG beam patterns.

3. RESULTS AND DISCUSSION

A. Mode-Locked Operation with a Fundamental Gaussian Beam

Initially, the passively mode-locked Tm:$LuYO_3$ ceramic laser was operated in the fundamental Gaussian mode employing collinear pumping. By slightly changing the separation between M2 and the Tm:$LuYO_3$ ceramic, two mode-locking regimes delivering femtosecond pulses of different durations were observed, both self-starting and stable for hours. In the first femtosecond regime, an average output power of 88 mW was obtained at 1.7 W of absorbed pump power, yielding a pulse energy of ~1.2 nJ. The optical spectrum centered at 2067 nm had an FWHM of 53 nm [see Fig. 2(a), dashed orange line], and the measured pulse duration amounted to 92 fs giving a time-bandwidth product (TBP) of 0.342. Slightly increasing the separation between M2 and the ceramic by roughly 0.5 mm, a second mode-locking region emerged for the same cavity configuration, with a lower output power of 51 mW but shorter pulse duration of 55 fs (66 fs before external compression in a 3-mm thick ZnS plate [30]), i.e., eight optical cycles, confirmed by recording the fringe-resolved interferometric autocorrelation function [see Fig. 2(b)]. In this case, the optical spectrum was broader (FWHM: 82 nm [29]) and centered at 2048 nm [solid orange line in Fig. 2(a)]. The corresponding TBP was calculated to be 0.322, very close to the value corresponding to bandwidth-limited $sech^2$-shaped pulses. Thus, although a secondary peak near 2200 nm was observed in the optical spectrum, presumably related to high-order dispersion, whose visibility was further enhanced by the leakage of the used OC [31], we believe that the second case represents true soliton mode-locking [32] and thus the pulse duration (τ_P) can be expressed as

$$\tau_P \propto |\mathrm{GDD}|/(\delta_L E_P). \quad (2)$$

At constant round-trip GDD, the pulse duration depends on the product of the intracavity pulse energy (E_P) and the self-phase modulation (SPM) coefficient (δ_L), where δ_L is inversely proportional to the mode area on the ceramic. By translating M2 from the first to the second femtosecond regime, the estimated mode area reduced roughly 2 times, thus leading to an enhancement of the SPM effect and further shortening of the pulse duration, very similar to previous observations in such mode-locked lasers [33,34]. The mode-area change can be also estimated from Eq. (2) using the measured output power and pulse duration in both cases. The result (a factor of 2.4) is rather close and the deviation can be attributed to nonlinear spatial effects such as self-focusing. Note that the beam radius on the SESAM increased only slightly from 120 to 140 μm when moving from the first to the second mode-locking region, which is a further indication that SPM is the primary mechanism responsible for the pulse shortening, while the SESAM, as a slow saturable absorber, initiates and stabilizes the mode-locking process. Finally, laser operation in the fundamental Gaussian mode was confirmed by the measured beam

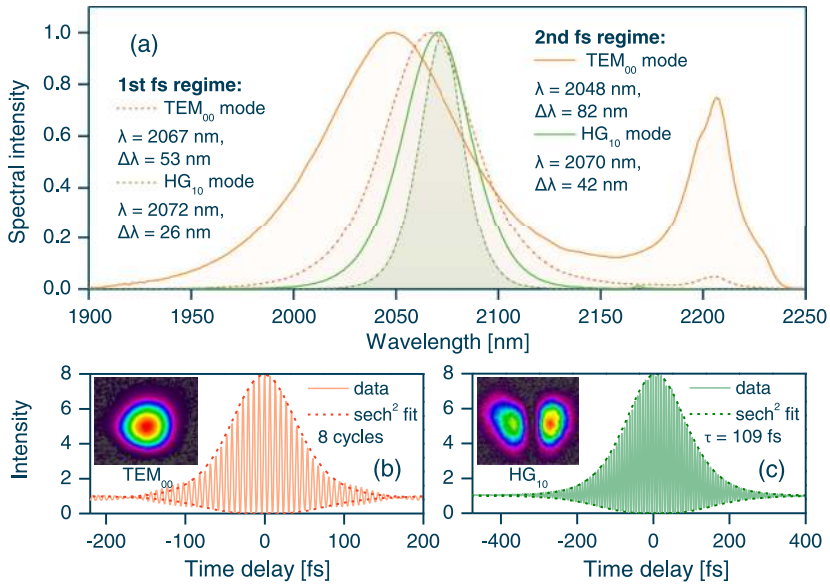

Fig. 2. (a) Optical spectra and (b), (c) interferometric autocorrelation traces of the mode-locked Tm : $LuYO_3$ ceramic laser operating in TEM_{00} and HG_{10} modes. Insets of (b) and (c) show the corresponding far-field beam patterns (fs, femtosecond).

pattern, as seen in the inset of Fig. 2(b), a typical TEM_{00} mode with negligible astigmatism.

B. Direct Generation of a Pulsed HG_{10} Mode in the Femtosecond Regime

Slightly off-axis pumping, achieved by minor shift of the pump beam along the X axis, supported the HG_{10} mode as expected. The latter originates from the laser threshold conditions, $P_{\text{th, min}} = \min\,[P_{\text{th}}(HG_{n,0})]$, derived by the mode overlap integral [35], since the HG_{10} mode exhibited the minimum threshold and thus oscillated first. Similar to the fundamental mode, mode-locking of the HG_{10} mode was also self-starting. However, the spectral FWHM was considerably narrower due to the weakened SPM effect resulting from the lower power and the two-lobe beam intensity distribution. In the first mode-locking region, an average output power of 48 mW was measured and the spectral FWHM amounted to 26 nm [see Fig. 2(a), dashed green line]. The pulse duration of 177 fs gave a TBP of 0.321. The corresponding beam pattern is shown in Fig. 3(b), a typical HG_{10} mode with two-lobe spatial intensity distribution. No adjacent transverse modes were observed, and the mode-locked operation was stable during the whole time of the experiment. The slight astigmatism of the beam pattern compared to that in the CW regime (a perfect HG_{10} beam profile) is attributed to the nonlinear astigmatism originating from the intensity-dependent Kerr lens effect.

Subsequently, translating M2 to reach the second mode-locking region, the beam pattern maintained the HG_{10} mode but exhibited asymmetric intensity distribution of the two lobes [see the inset of Fig. 2(c)]. The higher laser intensity of the lobe that better overlapped with the pump spot enhanced the SPM effect, thus leading to stronger nonlinear astigmatism but also enhanced spectral broadening. In this case, the spectral FWHM was 42 nm with a central wavelength at 2070 nm [see the solid green line in Fig. 2(a)]. By fitting the interferometric autocorrelation trace envelopes [see Fig. 2(c)] using a sech^2 function for the pulse shape, a pulse duration of 109 fs was obtained (TBP = 0.320). The exact 8:1 peak-to-background ratio and the perfect fitting indicate chirp-free pulse generation [36]. Mode-locking of yet higher-order $HG_{n,0}$ modes through increasing the pump offset was not achieved because of the inadequate spatial intensity distribution and the limited pump power.

C. Transformation to a Femtosecond LG_{01} Mode

As shown in Fig. 3(a), the HG_{10} output beam of the mode-locked laser was transformed to $LG_{0,\pm1}$ modes by a simple SCL converter. The middle and bottom rows in Fig. 3 show

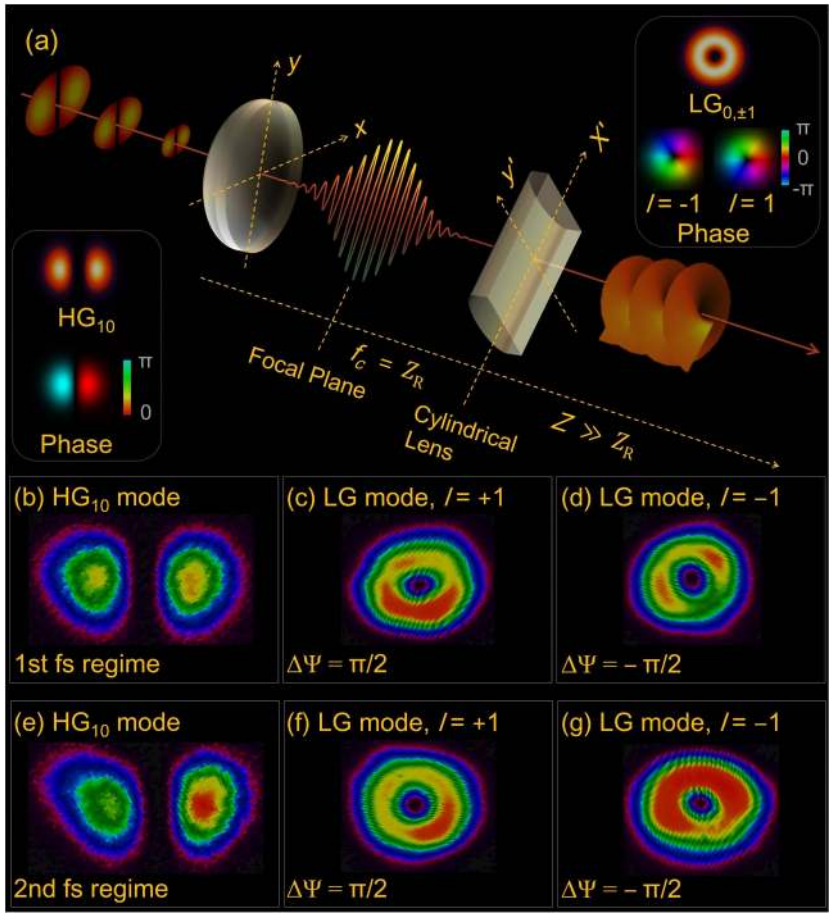

Fig. 3. (a) Schematic of the SCL mode converter, and the recorded far-field (b), (e) HG_{10} and (c), (d), (f), (g) $LG_{0,\pm1}$ beam patterns as the mode-locked laser operated in the first (middle row) and second (bottom row) femtosecond regimes (l, topological charge).

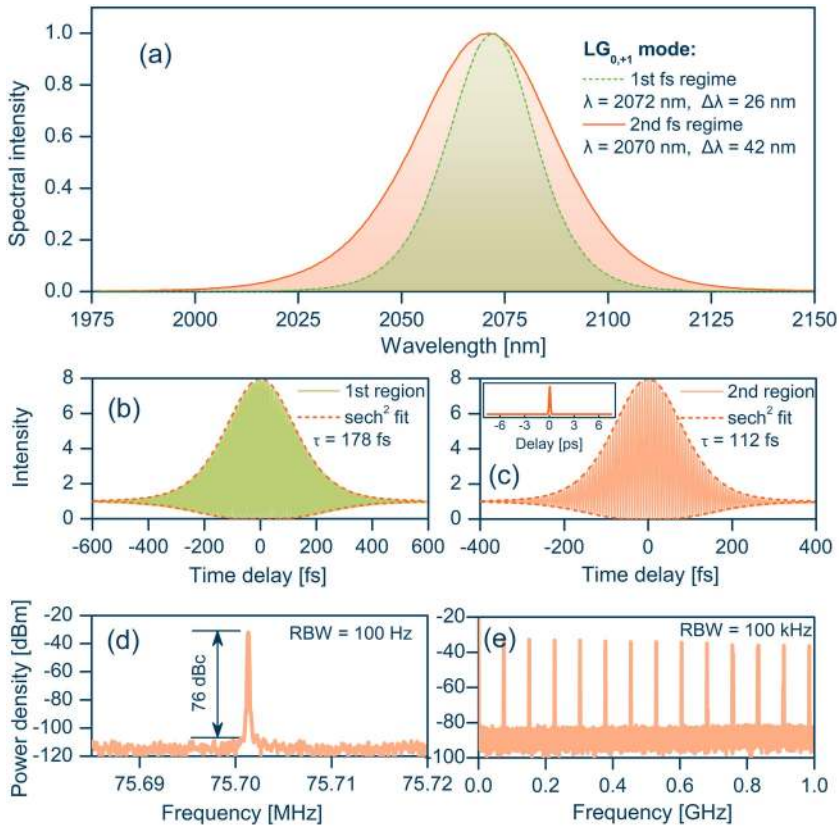

Fig. 4. (a) Optical spectrum of the generated $LG_{0,+1}$ modes and the corresponding interferometric autocorrelation traces in the (b) first and (c) second femtosecond regimes; (d) and (e) are the RF spectra of the femtosecond (112 fs) $LG_{0,+1}$ beam in different span ranges. The inset in (c) shows the noncollinear autocorrelation trace recorded on a long time scale (RBW, resolution bandwidth).

the measured HG_{10} and $LG_{0,\pm1}$ intensity patterns in the first and second femtosecond regimes, respectively. The imperfect circularity and the nonuniform spatial intensity distribution of the transformed $LG_{0,\pm1}$ modes [see Figs. 3(c), 3(d), 3(f), and 3(g)] were inherited from the HG_{10} mode. Nevertheless, the $LG_{0,\pm1}$ modes exhibited clean doughnut intensity profile without other high-order or mixed transverse modes. After passing through the converter, ~20% of the power was lost due to the uncoated cylindrical lens, resulting in average powers of 40 and 18 mW for the above-mentioned two regimes, respectively.

Subsequently, we investigated the spectral and temporal features of the femtosecond $LG_{0,\pm1}$ modes. No obvious difference was observed between these two modes whose characteristics are shown in Fig. 4. The spectra in the first and second femtosecond regimes exhibited no distortion or narrowing compared to the HG_{10} mode [see Figs. 4(a) and 2(a)], emphasizing the broadband conversion capability of the SCL converter used. The corresponding autocorrelation traces shown in Figs. 4(b) and 4(c), retained the $sech^2$ pulse profile with pulse durations of 178 and 112 fs, respectively. The slight pulse broadening in particular for the second femtosecond regime (from 109 to 112 fs), was caused by the negative GDD (~1000 fs^2 at 2.07 μm) of the 9-mm thick substrate material of the SCL converter. Nevertheless, the TBP in this case was 0.329, still very close to that of bandwidth-limited $sech^2$-shaped pulses. A clean single-pulse operation of the converted $LG_{0,+1}$ modes was confirmed by the noncollinear autocorrelation trace recorded on a long (±7.5 ps) time scale [see the inset of Fig. 4(c)]. Finally, the stability of the femtosecond vortex was characterized employing a radio frequency (RF) spectrum analyzer. From Fig. 4(d), the fundamental beat note with a high extinction ratio of 76 dBc above the noise level is an indication of a highly stable mode-locked regime. Moreover, the uniform harmonic beat notes free of additional modulations in a 1 GHz band [see Fig. 4(e)] are evidence of stable and clean pulsed LG mode without *Q*-switching instability or other transverse modes.

4. CONCLUSION

In conclusion, structured laser beams including the HG_{10} and $LG_{0,\pm1}$ modes were generated near 2 μm in the femtosecond regime employing a mode-locked solid-state laser and a simple SCL converter. No spatial chirp or topological-charge dispersion was introduced in contrast to the commonly used methods for producing ultrashort-pulse vortex beams [13–18]. The almost chirp-free pulses with smooth and broad optical spectra are evidence for the high reliability of the oscillator and the converter. On one hand, this work demonstrates the shortest high-order transverse mode pulses directly generated by a mode-locked solid-state laser, and on the other it shows the first ~100 fs optical vortices in the 2-μm spectral range. It confirms the unique capability of such laser systems to generate ultrashort-pulse SLBs with broad optical spectrum but without unwanted chirp. We believe the present achievement paves the way for generating

few-cycle pulse optical vortices at 2 μm, e.g., through enhancing the SPM effect since 55 fs (eight optical cycles) has been already achieved in the fundamental Gaussian mode in the present cavity configuration. Finally, the stable femtosecond laser vortices obtained near 2 μm can be employed to generate optical vortex infrared supercontinuum, as a seed for straightforward power scaling using novel single crystal fibers and HHG generation, special microstructuring of transparent materials, and mid-IR vortex generation through nonlinear frequency downconversion.

Funding. National Natural Science Foundation of China (51761135115, 52032009, 61975208, 62075090); Deutsche Forschungsgemeinschaft (PE 607/14-1); Laserlab-Europe (654148); Natural Science Foundation of Jiangsu Province (BK20190104); Sino-German Scientist Cooperation and Exchanges Mobility Programme (M-0040); Alexander von Humboldt-Stiftung.

Acknowledgment. We thank Dr. J. Zhang from Key Laboratory of Transparent and Opto-Functional Inorganic Materials, Shanghai Institute of Ceramics, China, for the Tm:$LuYO_3$ ceramic, and M. Guina from Reflektron Ltd., Tampere, Finland, for the SESAM used in the present study. Y. Zhao acknowledges financial support from the Alexander von Humboldt Foundation through a Humboldt fellowship.

Disclosures. The authors declare no conflicts of interest.

REFERENCES

1. A. Forbes, "Structured light from lasers," Laser Photonics Rev. **13**, 1900140 (2019).
2. E. J. Bochove, G. T. Moore, and M. O. Scully, "Acceleration of particles by an asymmetric Hermite-Gaussian laser beam," Phys. Rev. A **46**, 6640–6653 (1992).
3. H. S. Ghotra and N. Kant, "TEM modes influenced electron acceleration by Hermite-Gaussian laser beam in plasma," Laser Part. Beams **34**, 385–393 (2016).
4. L. Allen, M. W. Beijersbergen, R. J. C. Spreeuw, and J. P. Woerdman, "Orbital angular-momentum of light and the transformation of Laguerre-Gaussian laser modes," Phys. Rev. A **45**, 8185–8189 (1992).
5. D. G. Grier, "A revolution in optical manipulation," Nature **424**, 810–816 (2003).
6. J. Wang, I. M. F. J. Yang, N. Ahmed, Y. R. Y. Yan, H. Huang, Y. Yue, S. Dolinar, M. Tur, and A. E. Willner, "Terabit free-space data transmission employing orbital angular momentum multiplexing," Nat. Photonics **6**, 488–496 (2012).
7. K. I. Willig, S. O. Rizzoli, V. Westphal, R. Jahn, and S. W. Hell, "STED microscopy reveals that synaptotagmin remains clustered after synaptic vesicle exocytosis," Nature **440**, 935–939 (2006).
8. A. Mair, A. Vaziri, G. Weihs, and A. Zeilinger, "Entanglement of the orbital angular momentum states of photons," Nature **412**, 313–316 (2001).
9. P. Polynkin, C. Ment, and J. V. Moloney, "Self-focusing of ultraintense femtosecond optical vortices in air," Phys. Rev. Lett. **111**, 023901 (2013).
10. M. Zürch, C. Kern, P. Hansinger, A. Dreischuh, and C. Spielmann, "Strong-field physics with singular light beams," Nat. Phys. **8**, 743–746 (2012).
11. N. M. Litchinitser, "Structured light meets structured matter," Science **337**, 1054–1055 (2012).
12. J. Ni, C. Wang, C. Zhang, L. Y. Y. Hu, Z. Lao, J. L. B. Xu, D. Wu, and J. Chu, "Three-dimensional chiral microstructures fabricated by structured optical vortices in isotropic material," Light Sci. Appl. **6**, e17011 (2017).
13. K. Bezuhanov, A. Dreischuh, G. G. Paulus, M. G. Schatzel, and H. Walther, "Vortices in femtosecond laser fields," Opt. Lett. **29**, 1942–1944 (2004).
14. I. G. Mariyenko, J. Strohaber, and C. J. G. J. Uiterwaal, "Creation of optical vortices in femtosecond pulses," Opt. Express **13**, 7599–7608 (2005).
15. K. J. Moh, X.-C. Yuan, D. Y. Tang, W. C. Cheong, L. S. Zhang, D. K. Y. Low, X. Peng, H. B. Niu, and Z. Y. Lin, "Generation of femtosecond optical vortices using a single refractive optical element," Appl. Phys. Lett. **88**, 091103 (2006).
16. M. Bock, J. Brunne, A. Treffer, S. König, U. Wallrabe, and R. Grunwald, "Sub-3-cycle vortex pulses of tunable topological charge," Opt. Lett. **38**, 3642–3645 (2013).
17. R. Grunwald, T. Elsaesser, and M. Bock, "Spatio-temporal coherence mapping of few-cycle vortex pulses," Sci. Rep. **4**, 7148 (2015).
18. I. Zeylikovich, H. I. Sztul, V. Kartazaev, T. Le, and R. R. Alfano, "Ultrashort Laguerre-Gaussian pulses with angular and group velocity dispersion compensation," Opt. Lett. **32**, 2025–2027 (2007).
19. H. A. Nam, M. G. Cohen, and J. W. Noe, "A simple method for creating a robust optical vortex beam with a single cylinder lens," J. Opt. **13**, 064026 (2011).
20. M. W. Beijersbergen, L. Allen, H. E. L. O. van der Veen, and J. P. Woerdman, "Astigmatic laser mode converters and transfer of orbital angular-momentum," Opt. Commun. **96**, 123–132 (1993).
21. R. Uren, S. Beecher, and W. A. Clarkson, "Method for generating high purity Laguerre–Gaussian vortex modes," IEEE J. Quantum Electron. **55**, 1700109 (2019).
22. D. E. Spence, P. N. Kean, and W. Sibbett, "60-fsec pulse generation from a self-mode-locked Ti:sapphire laser," Opt. Lett. **16**, 42–44 (1991).
23. H. C. Liang, Y. J. Huang, Y. C. Lin, T. H. Lu, Y. F. Chen, and K. F. Huang, "Picosecond optical vortex converted from multigigahertz self-mode-locked high-order Hermite–Gaussian Nd:$GdVO_4$ lasers," Opt. Lett. **34**, 3842–3844 (2009).
24. S. Zhang, P. Li, S. Wang, J. Tan, G. Feng, and S. Zhou, "Ultrafast vortices generation at low pump power and shearing interferometer-based vortex topological detection," Laser Phys. Lett. **16**, 035320 (2019).
25. Z. Qiao, L. Kong, G. Xie, Z. Qin, P. Yuan, L. Qian, X. Xu, J. Xu, and D. Fan, "Ultraclean femtosecond vortices from a tunable high-order transverse-mode femtosecond laser," Opt. Lett. **42**, 2547–2550 (2017).
26. H. Tong, G. Xie, Z. Qiao, Z. Qin, P. Yuan, J. Ma, and L. Qian, "Generation of a mid-infrared femtosecond vortex beam from an optical parametric oscillator," Opt. Lett. **45**, 989–992 (2020).
27. J. Paajaste, S. Suomalainen, A. Härkönen, U. Griebner, G. Steinmeyer, and M. Guina, "Absorption recovery dynamics in 2 μm GaSb-based SESAMs," J. Phys. D **47**, 065102 (2014).
28. Y. Zhao, L. Wang, Y. Wang, J. Zhang, X. X. P. Liu, Y. Liu, D. Shen, J. E. Bae, T. G. Park, F. Rotermund, X. Mateos, P. Loik, Z. Wang, X. Xu, J. Xu, M. Mero, U. Griebner, V. Petrov, and W. Chen, "SWCNT-SA mode-locked Tm:$LuYO_3$ ceramic laser delivering 8-optical-cycle pulses at 2.05 μm," Opt. Lett. **45**, 459–462 (2020).
29. Y. F. Chen, Y. H. Lai, M. X. Hsieh, Y. H. Hsieh, C. W. Tu, H. C. Liang, and K. F. Huang, "Wave representation for asymmetric elliptic vortex beams generated from the astigmatic mode converter," Opt. Lett. **44**, 2028–2031 (2019).
30. Y. Zhao, L. Wang, Z. Pan, Y. Wang, J. Zhang, P. Liu, X. Xu, D. Shen, J. Xu, S. Suomalainen, A. Härkönen, M. Guina, P. Loiko, X. Mateos, U. Griebner, V. Petrov, and W. Chen, "Sub-60 fs SESAM mode-locked Tm:$LuYO_3$ ceramic laser," in *Conference on Lasers and Electro-Optics/Europe and the European Quantum Electronics Conference* (OSA, 2019), paper CA-6.2.
31. Y. Zhao, L. Wang, W. Chen, Z. Pan, Y. Wang, P. Liu, X. Xu, Y. Liu, D. Shen, J. Zhang, M. Guina, X. Mateos, P. Loiko, Z. Wang, X. Xu, J. Xu, M. Mero, U. Griebner, and V. Petrov, "SESAM mode-locked Tm:$LuYO_3$ ceramic laser generating 54 fs pulses at 2048 nm," Appl. Opt. **59**, 10493–10497 (2020).
32. U. Keller, "Ultrafast solid-state lasers," Prog. Opt. **46**, 1–115 (2004).

33. Y. Zhao, Y. Wang, X. Zhang, X. Mateos, Z. Pan, P. Loiko, W. Zhou, X. Xu, J. Xu, D. Shen, S. Suomalainen, A. Härkönen, M. Guina, U. Griebner, and V. Petrov, "87 fs mode-locked Tm,Ho:$CaYAlO_4$ laser at ~2043 nm," Opt. Lett. **43**, 915–918 (2018).
34. A. A. Lagatsky, X. Han, M. D. Serrano, C. Cascales, C. Zaldo, S. Calvez, M. D. Dawson, J. A. Gupta, C. T. A. Brown, and W. Sibbett, "Femtosecond (191 fs) $NaY(WO_4)_2$ Tm,Ho-codoped laser at 2060 nm," Opt. Lett. **35**, 3027–3029 (2010).
35. Y. F. Chen, T. M. Huang, C. F. Kao, C. L. Wang, and S. C. Wang, "Generation of Hermite-Gaussian modes in fiber-coupled laser-diode end-pumped lasers," IEEE J. Quantum Electron. **33**, 1025–1030 (1997).
36. J.-C. M. Diels, J. J. Fontaine, I. C. McMichael, and F. Simoni, "Control and measurement of ultrashort pulse shapes (in amplitude and phase) with femtosecond accuracy," Appl. Opt. **24**, 1270–1282 (1985).